CHAPTER

Fundamentals of immiscible polymer blends 4

4.1 Introduction

The blending of two or more dissimilar polymers with different chemical structures and molecular weights has become a fast, attractive, and cost-effective method from an industrial point of view for the fabrication of new materials with intermediate properties [1]. However, it should be borne in mind that the thermodynamic aspects associated with polymers leads to the formation of phase-separated structures and different morphologies in polymer blends depending on the extent of the polymer–polymer interactions. This allows manufacturers and researchers to tailor the properties of blends by tuning the morphologies with respect to their intended applications. The cost–performance ratio in fabrication of polymer blends compared with synthesis of new material is an advantage of blending for commercialization of products. With regard to mass production however, melt blending is considered more convenient, cheaper, and less hazardous than solvent casting. The latter technique requires a great amount of solvent which is not economically favored in mass production. Plus, some solvent may still remain inside the product at the end of the process, which could be considered as a defect. Although blending seems a promising route in the production of materials with various interesting properties; understating of the polymer–polymer interactions and different morphologies remains challenging since a series of different parameters come into play in defining the structures of the fabricated blends [2]. Considering that the polymer pairs are immiscible in most cases, the effect of flow during mixing (processing), temperature, blend compositions, chemistry of the polymers (molecular weights, glass transition temperatures, melting point, solubility, etc.), and interfacial properties can alter the morphologies and thus final properties. Hence, a great deal of investigations have been carried out on the relationships between the structure properties of blends.

4.2 Phase behavior

Having said that different structures can be made depending on the thermodynamic aspects of the polymer pairs, it is of importance to understand the basics of the phase separations in polymer blends. In context with discussion on the miscibility of the

Nanostructured Immiscible Polymer Blends. https://doi.org/10.1016/B978-0-12-816707-6.00004-3

polymers, Utracki et al. [1] classified the polymer blends with respect to their phase structures as follows:

- Miscible blends: those polymer blends which behave as a single-phase material and show homogeneity at a macroscopic (molecular) scale.
- Immiscible blends: This refers to those polymer blends having phase-separated structures at all compositions and temperatures with phases having the same characteristics as those of the components before blending.
- Partially miscible blends: This class of polymer blends refers to those blends that are miscible within a range of temperatures and compositions.

It has been reported that phase separation could be a result of low miscibility or crystallization of one of the phases [3]. This, in turn, would give rise to different phase diagram behaviors (Fig. 4.1). However, it has been shown that most high-molecular-weight polymer pairs are partially miscible, showing lower critical solution temperature (LCST) behavior as a result of entropy effects [1,3].

A polymer blend is miscible when the Gibbs free energy of a mixture ΔG_m (Eq. 4.1) is negative ($\Delta G_m<0$),

$$\Delta G_m = \Delta H_m - T\Delta S_m \tag{4.1}$$

where $\left(\frac{\partial^2 \Delta G_m}{\partial \varnothing^2}\right)_{T,P} > 0$ at constant temperature and pressure. ΔH_m and ΔS_m are the enthalpy and entropy of mixing, respectively. Given the abovementioned definitions and different possible morphologies of the blends depending on the intermolecular

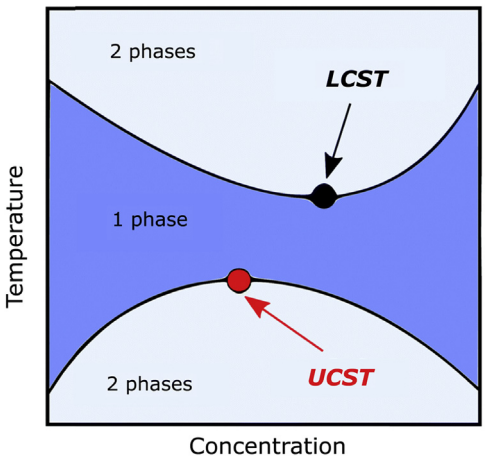

FIGURE 4.1

Upper and lower critical solution temperatures (UCST) and (LCST) behaviors of polymers shown in a phase diagram [4].

interactions, unraveling the window of miscibility is important. The most common method is to apply the Flory–Huggins theory (Eq. 4.2) to obtain the phase diagram of the blends at different temperatures and compositions.

$$\Delta G_m = RT(n_1 \ln \varnothing_1 + n_2 \ln \varnothing_2 + n_1 \varnothing_2 \chi_{12}), \tag{4.2}$$

in which R is the gas constant, T is the absolute temperature, $\varnothing$ is the volume fraction of the component, n is the number of moles, and χ is the interaction parameter between components.

4.3 Morphology development

It has been discussed that properties of the blends can be tuned by adjusting the blend morphology through composition change, interfacial tensions, and processing conditions. Therefore, it is important to understand the morphology of the blends with respect to the parameters affecting the structures. Some of the major morphology types attained on blending are: (1) droplet–matrix morphology; (2) cylindrical or fibrous morphology; (3) layered or lamellar morphology; and (4) co-continuous morphology. Wu et al. [5] expressed that by changing the volume ratios of the polylactide/poly(ε-caprolactone) PLA/PCL blends the aforementioned morphologies can be obtained (Fig. 4.2). However, it is necessary to consider that viscosity ratios of the component play a significant role in determination of the obtained morphology.

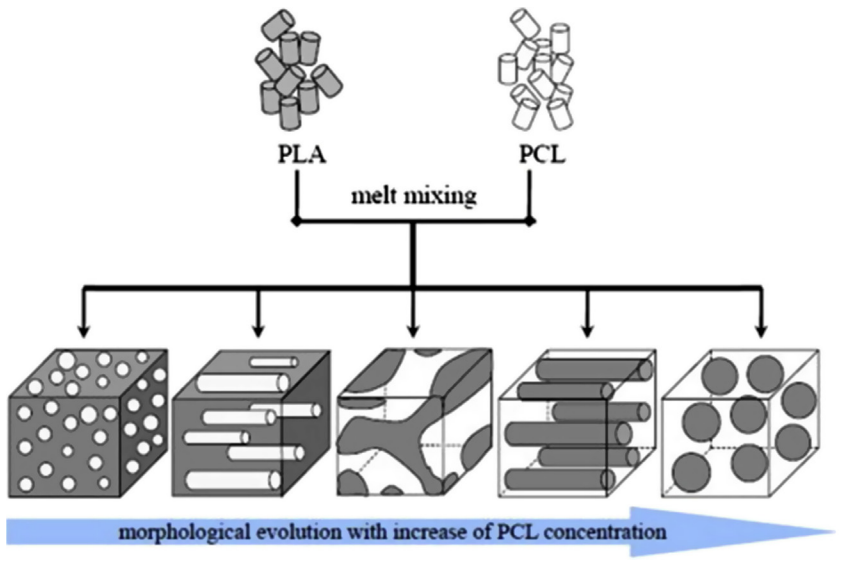

FIGURE 4.2

Cartoon illustrating the morphological changes in PLA/PCL blends when the PCL concentration is increased [5].

As will be discussed, the viscosity ratio has an impressive effect on the capillary number $\left(Ca = \frac{\tau}{\alpha/R} = \frac{\eta_m \dot{\gamma} R}{\alpha}\right)$ and hence on the breakup of the droplets in polymer blends.

In an immiscible blend a decrease in viscosity ratio (η_d/η_m, where $\eta_m$and η_d are viscosity of the matrix and dispersed phase, respectively) affords the breaking up of a droplet during the flow of the mixture through the extension of a droplet into a thread and eventually it raptures [6,7]. It can be observed that the two hydrodynamic forces (τ) and cohesive forces (α/R, with α as interfacial tension and R being droplet radius) control the droplet deformations first by applying shear stress and also by restoring the stress through an interfacial tension, respectively. Therefore, there is a balance between these two forces which determines the droplet deformation where it is demonstrated by the capillary number (Ca). It is worth mentioning that in systems where a high viscous phase (droplet) is dispersed in a less viscous matrix, breakup and deformation of the droplet are hindered. This could lead to larger droplet size with broad distributions [8,9]. Favis and Therrien [9] found that at high viscosity ratios and compositions of polypropylene/polycarbonate (PP/PC) blends, fibrous morphologies can be formed where droplet sizes become larger as composition is increased. It should be noted that breakup and coalescence of droplets are the major phenomena dictating the morphology developments in immiscible polymer blends [10]. It was discussed that depending on the applied shear stress and viscosity ratio of the components a droplet can be stretched and eventually breakup into smaller droplets through a Rayleigh instability mechanism [11]. This occurs when the shear stress τ overcomes the interfacial tension α at capillary numbers larger than the critical capillary number. Meanwhile, coalescence of the dispersed phase droplets is another factor governing the morphology evolutions. Generally, droplets can collide during the flow or by Brownian motion in a stagnant condition [12]. When the collision happens the matrix film between the two approaching droplets is removed and thus raptures at the extreme thinnest portion at film thicknesses below the critical value h_c. Eventually the droplets merge into a bigger droplet which can undergo another breakup process later during the flow, indicating that there is an equilibrium in breakup and coalescence during mixing which determines the final droplet size [11,13,14]. In view of the foregoing discussions, different models have been developed to define the limits of the coalescence and breakup with respect to the mobility of the interface allowing the formation of morphological hysteresis [15,16]. Such models, namely partially mobile interface (PMI), fully mobile interface (FMI), and immobile interface (IMI), indicate the important role of the interface in defining the morphology of an immiscible polymer blend. It should be noted that breakup and coalescence are also dependent on the residence time of the droplet under the stress as well as on the volume fraction of the dispersed phase droplets [13]. At a sufficient given residence time morphologies can be homogeneous due to the equilibrium between coalescence and breakup. Moreover, larger droplets require a longer time to coalesce as the film drainage takes longer. In general, it can be understood that different parameters such as shear stress, viscosity ratio, dispersed phase concentration, and interfacial tension are involved in morphology evolutions.

4.3.1 Phase continuity and blend composition

It was discussed that depending on the abovementioned parameters different morphology types can be obtained. Among the different morphologies the co-continuous structures gained more attention owing to their superior properties of combination of the two components than in the droplet−matrix morphology [17−20]. By definition, a co-continuous morphology is a structure where the continuous minor phase is interconnected within a continuous matrix [19,21]. The co-continuous morphology allows the designing of conductive polymer blends or if the second phase is etched it can be used in scaffolds for tissue engineering applications [22,23]. It has been also shown that this type of morphology can be found near the phase-inversion concentrations. That is, further changing the concentration can inverse the matrix phase into the dispersed phase. Moreover, it was declared that morphology types are highly dependent on the viscosity of the components. Avgeropoulos et al. [24] reported that in order to attain the co-continuous morphology in a (50/50 w/w) butadiene rubber/ethylene propylene diene monomer (BR/EPDM) the melt mixing viscosities of both polymers need to be equal. Hereafter, many efforts have been made to predict and model the phase-inversion morphology according to the rheological methods summarized in Table 4.1. It can be observed that some of the models are based on the viscosity ratios. The viscosity ratios are normally calculated at constant shear rates which can lead to discrepancies in the results. Shear rate changes, as does the viscosity ratio at the corresponding shear rate. It is worth remembering that stress profiles can be different and nonuniform during processing. Hence, the predicted phase inversion composition based on viscosity ratio models may not be completely accurate [21]. It must be noted that in the case of immiscible polymer blends the interface plays a crucial role in morphology evolutions since there are interfacial tensions between the two phases. Therefore, not only viscosity ratios but also elasticity of the components can significantly affect the morphology. In fact, the elasticity effect was found to be even more determinant since interfacial contributions are also included. It has been reported that in sufficiently given concentrations the more elastic component could enfold the other component having less elasticity, forming a continuous matrix phase [7,21]. However, Steinmann et al. [32] expressed that the elasticity ratio could relate to the viscosity ratio and cannot be an independent factor. Thus, concluding it may not be applicable to a broad range of blends.

In light of the abovementioned reasons efforts have been made to include the elasticity and parameters associated with it, such as interfacial tension or droplet (pore) sizes as well. Vanoene [33] developed an equation taking into account the effect of interfacial tensions as follows:

$$\alpha_{md} = \alpha^0_{md} + R/6\left[N_{2,d} - N_{2,m}\right], \tag{4.13}$$

in which α_{md} and α^0_{md} are the interfacial tensions between the matrix and dispersed phase during and in the absence of flow, respectively. R is the radius of the dispersed

Table 4.1 Summary of some of the models developed to predict the phase-inversion morphology of immiscible blends.

Model	Equation	Blends	References
$\frac{\phi_1}{\phi_2} = \frac{\eta_1}{\eta_2}$	4.3	BR/EPDM General	Avgeropoulos [24], Paul-Barlow [2]
$\frac{\phi_1}{\phi_2} = 1.22\left[\frac{\tau_1}{\tau_2}\right]^{0.29}$	4.4	PP/EPR PS/SBR	Ho et al. [25]
$\frac{\phi_1}{\phi_2} = 0.887\left[\frac{\tau_1}{\tau_2}\right]^{0.29}$	4.5	PA/SAN	Kitayama et al. [26]
$\frac{\phi_1}{\phi_2} = 1.59\left[\frac{\tau_1}{\tau_2}\right]^{0.19}$	4.6	PP/PS	Omonov et al. [27]
$\frac{\phi_1}{\phi_2} = \left[\frac{\eta_1}{\eta_2}\right]^{0.3}$	4.7	PP/(PS/PPE)	Everaert et al. [28]
$\eta_2 = \eta_1\left[1 - \frac{\phi_2}{\phi_m}\right]^{-[\eta_2]\phi_m}$	4.8	Latex suspensions	Krieger-Dougherty [29]
$\lambda = \left[\frac{(\phi_m/\phi_2)}{(\phi_m/\phi_1)}\right]^{[\eta]\phi_m}$	4.9	General	Utracki [30]
$\phi_2 = \frac{1-\log\lambda^{\frac{\lambda}{[\eta]}}}{2},\ [\eta] = 1.9$			
$\phi_2 = \left[1 + \frac{\eta_1}{\eta_2}\left[1 + 2.25\log\left(\frac{\eta_1}{\eta_2}\right) + 1.81\left(\log\left(\frac{\eta_1}{\eta_2}\right)\right)^2\right]\right]^{-1}$	4.10	General	Metelkin-Blekht [31]
$\phi_2 = -0.12\log\left(\frac{\eta_1}{\eta_2}\right) + 0.48$	4.11	PMMA/PS PMMA/PSAN	Steinmann et al. [32]
$\frac{\phi_1}{\phi_2} = \frac{G_2'}{G_1'}$	4.12	PS/HDPE	Bourry-Favis [21]

ϕ *and* η *are the volume fraction and viscosity of the components, respectively.* $[\eta_2]$ *is the intrinsic viscosity of the latex spheres.* ϕ_m *is the maximum packing volume fraction.* τ *is the torque values.* G′ *is the elastic modulus of the components.* EPR, *ethylene propylene rubber,* SBR, *styrene butadiene rubber,* PS, *polystyrene,* PA, *polyamide,* SAN, *styrene acrylonitrile,* PPE, *poly(dimethyl phenylene ether),* PMMA, *poly(methyl methacrylate),* PSAN, *radically synthesized polystyrene acrylonitrile,* HDPE, *high-density polyethylene.*

This table is adapted from Pötschke, P., Paul, D. Formation of co-continuous structures in melt-mixed immiscible polymer blends. Journal of Macromolecular Science: Part C: Polymer Reviews 2003;43:87–141; Omonov, T., Harrats, C., Groeninckx, G., Moldenaers, P. Anisotropy and instability of the co-continuous phase morphology in uncompatibilized and reactively compatibilized polypropylene/polystyrene blends. Polymer 2007;48:5289–5302.

droplet, $N_{2,d}$ and $N_{2,m}$ are the second normal stress differences of the dispersed phase and matrix, respectively.

Willemse et al. [34] proposed a model taking into account the interfacial tension α and filament dimensions, describing the co-continuous morphology (Eq. 4.14) when the capillary number is 1 (Ca = 1).

$$\frac{1}{\phi_{dispersed}} = 1.38 + 0.0213\left(\frac{\eta_m \dot{\gamma}}{\alpha} R_0\right)^{4.2} \tag{4.14}$$

where $\dot{\gamma}$ is the shear rate, η_m is the matrix viscosity, and $\phi_{dispersed}$ is the minimum volume fraction of the second phase where a co-continuous morphology can be found. Although the models can be used to explain the effect of processing conditions on the co-continuous morphology ranges, it cannot be used as a predictive tool since the filament (droplet) diameter needed to be calculated afterward. Another way of characterizing the co-continuous morphologies is to use small-amplitude oscillatory shear (SAOS) tests as they are quite sensitive to the morphologies of the blends. In many researches the elastic (storage) modulus G′ (ω) has been used as an indication of morphology change [5,35–37]. It has been shown that blends with co-continuous structures showing a power law behavior have a maximum G′ (ω) at low frequencies [5,38,39]. In other words, blends with co-continuous or near phase-inversion morphologies show the highest elasticity. This enhancement in elastic modulus of the co-continuous blends is due to the development of interfacial areas, hence providing stronger interactions at the interface [38,39]. On the other hand, blends with droplet–matrix morphology demonstrate a shoulder (plateau modulus) at low-frequency regions associated with the shape (form) relaxation process of the deformed dispersed phase droplets [39,40]. From these discussions it can be understood that the interface has an inevitable contribution in morphology development of immiscible blends. Therefore, analyzing the interfacial properties could be quite informative in understanding the microstructure of blends. Thus, the modulus of a blend G^*_{blend} can be written as a combination of those of the component $G^*_{components}$ and interface $G^*_{interface}$ contributions as follows [41]:

$$G^*_{blend} = G^*_{components} + G^*_{interface} \tag{4.15}$$

Yu et al. [41] adopted the model (Eq. 4.16) originally developed by Veenstra et al. [42] for modeling of the Young's modulus of the co-continuous blends to be used for prediction of the dynamic complex modulus of the components $G^*_{components}$.

$$G^*_{components} = \frac{\alpha'^2 b' G_1^{*2} + \left(\alpha'^3 + 2\alpha' b' + b'^3\right) G_1^* G_2^* + \alpha' b'^2 G_2^{*2}}{b' G_1^* + a' G_2^*} \tag{4.16}$$

where $3\alpha'^2 - 2\alpha'^3 = \varnothing_1$ is the volume fraction of component 1, with α' and b' describing the average reduced length of components 1 and 2 correspondingly, and $b' = 1 - a'$. Therefore, the interfacial contribution of the dynamic complex modulus $G^*_{interface}$ can be obtained if Eq. (4.16) is resolved. In the case of droplet–

matrix morphology the emulsion model of Palierne (Eqs. 4.17 and 4.18) has been frequently used to calculate the interfacial tensions of the blends [5,40,43–46].

$$G_b^* = G_m^* \frac{1 + 3\int_i^\infty \varnothing H(\omega)}{1 - 2\int_i^\infty \varnothing H(\omega)} \tag{4.17}$$

where,

$$H(\omega) = \frac{4\left(\frac{\alpha}{R_v}\right)\left[2G_m^*(\omega) + 5G_d^*(\omega)\right] + \left[G_d^*(\omega) - G_m^*(\omega)\right]\left[16G_m^*(\omega) + 19G_d^*(\omega)\right]}{40\left(\frac{\alpha}{R_v}\right)\left[G_m^*(\omega) + G_d^*(\omega)\right] + \left[2G_d^*(\omega) + 3G_m^*(\omega)\right]\left[16G_m^*(\omega) + 19G_d^*(\omega)\right]}, \tag{4.18}$$

$\varnothing$, ω, R_v, and α are droplet volume fraction, angular frequency, volume-average radius of droplet, and interfacial tension, respectively. G_m^*, G_d^*, and G_b^* represent the complex moduli of the polymer matrix, dispersed phase, and blend, respectively. By fitting the modulus of the blends with the Palierne model the interfacial tension can be acquired. However, it must be noted that in the calculations the use of volume-average droplet size may cause some uncertainty in the results since in practice there is a distribution of droplet sizes. Therefore, it may be more suitable to systems with narrow distributions (less than 2) and assuming the interfacial tension is constant and independent of the interfacial area [5,40,44,45]. The weighted relaxation spectrum $\tau H(\tau)$ is another useful tool for characterizing the morphology of blends. There are different methods for calculation of continuous relaxation spectra [47–50]. In general, the peak appearing at longer times (low frequencies) is associated with the shape (form) relaxation time of the droplets and those at shorter times (high frequencies) are associated with relaxation of the component chains [51,52]. It has been shown in the case of co-continuous blends the spectra at longer times appear as a tail (not fully relaxed) due to the larger interfacial areas requiring much longer time than the experimental window to be relaxed (Fig. 4.3) [45,53,54].

4.4 Morphology coarsening and compatibilization

Thus far the important role of the interface in morphology development of immiscible blends has been clearly explained. Moreover, it was discussed that coalescence is an inevitable phenomenon in immiscible blends. This again reflects the role of interfacial properties in stabilizing the morphologies. At this point, it would be better to discuss the matter with respect to the different morphologies. It should be noted that in co-continuous blends the excessive stored energy at the interfacial areas leads to thermodynamically unstable structures [19,20,53]. This, in turn, will cause coarsening of the phase which is companied by a reduction in the elastic modulus G' (ω) of the blends. On the other hand, in the case of the droplet–matrix morphology type of blend the final properties are proportional to the average droplet size and droplet

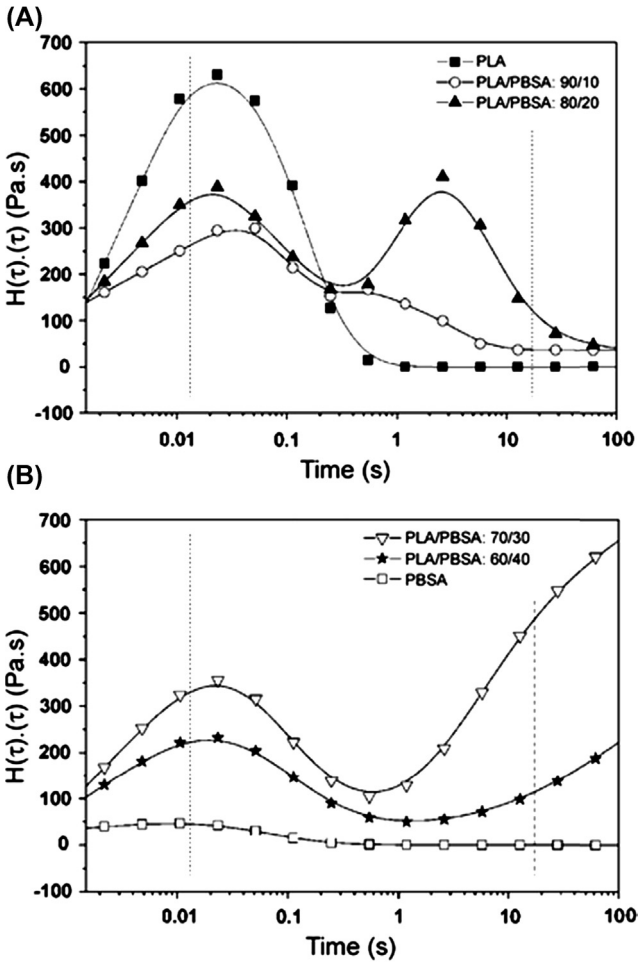

FIGURE 4.3

Weighted relaxation spectra of the (A) (90/10), (80/20) and (B) (70/30), (60/40) PLA/PBSA blends acquired at 175°C. (A) The relaxation spectra of the droplet–matrix morphology and (B) the weighted spectra of the morphologies with large droplets or co-continuous structures [45].

size distributions. Blends with smaller droplet size and narrow distributions exhibit superior characteristics to those with large droplets with broad distributions. Therefore, interfacial stabilizers known as "compatibilizers" have been incorporated into the blends in order to reduce the coarsening of the phase-separated structures. The so-called "compatibilizers" can be incorporated into the blends before blending (ex situ compatibilization) or can be obtained through reactive processing during the

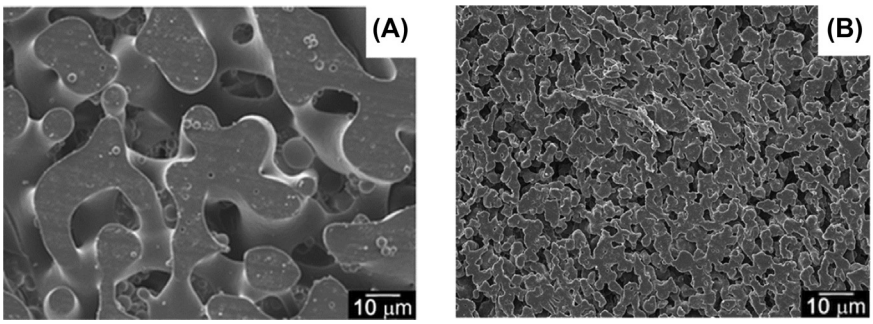

FIGURE 4.4

Scanning electron microscopy (SEM) images of the 50/50 vol.% (A) PE/PEO and (B) compatibilized PE-g-MA/PEO blends [19].

Reproduced with permission from the American Chemical Society (ACS). Copyright 2012.

blending at the interface (in situ compatibilization) [6,10]. In an in situ compatibilization interfacial tension is reduced when a copolymer is generated at the interface as a result of chemical reactions such as Friedel–Crafts alkylation, transesterification, hydrogen bonding, etc. [55–57]. Fig. 4.4 shows the compatibilization of 50/50 vol.% polyethylene/poly(ethylene oxide) (PE/PEO) blend by replacing PE with maleic anhydride grafted polyethylene (PP-g-MA).

It has been reported that the anhydride group of the PP-g-MA reacts with the OH group of PEO, thus reducing the interfacial tension and corresponding dispersed phase size. In the case of classical ex situ compatibilization, block or graft copolymers having compatible molecules with both components are added to the blends creating a bridge between the two phases. The copolymer at the interface reduces the interfacial tension by retarding the film drainage at the interface, thus immobilizing the interface [6]. On the other hand, at sufficient concentrations copolymers can cover the surface of the droplets and create a core–shell structure whereby coalescence of the droplets can be suppressed due to the repulsive forces [58].

4.5 Inorganic interfacial modifiers

The use of inorganic nanoparticles in polymers has been growing recently due to their superior mechanical, thermal, barrier, and electrical properties. This is also the case with regard to immiscible polymer blends, which are the scope of this book. However, it is worth mentioning that the extent of property improvement in the case of nanoparticle-incorporated polymer blends is proportional to the localization and distribution of the nanoparticles within the blend [59]. Therefore, nanoparticles can contribute to the stabilization of morphologies with respect to different localizations. At this point we point out the mechanisms involved in stabilization of the microstructures in nanoparticle-filled immiscible polymer blends.

1. When nanoparticles are localized in the continuous matrix phase having the higher concentrations the viscosity ratio decreases, leading to droplet breakup due to the facilitation of stress transfer to the dispersed phase droplets [28,60].
2. Interfacial localization of nanoparticles could suppress the coalescence of the two neighboring droplets due to the steric repulsion effect. The most efficient result can be obtained when the interface is covered with sufficient nanoparticles [61–64]. It has also been found that the state of the exfoliation/intercalation at the interface can affect the size reduction, whereas nanoclays that were distributed evenly could have a more significant influence on size reduction [65].
3. "Cutting effect" is another mechanism proposed by Zhu et al. [66] to account for the size reduction. In such a case which is limited to the plate-like nanoparticles such as clays and graphene-based nanoparticles, at some critical concentration nanoparticles form a "knife-like" structure that can cut the hosting dispersed phase droplets having the lower concentration [67–69]. In general, when nanoparticles are localized inside the droplets in a droplet–matrix morphology blend, they can increase the viscosity ratio of the blend and therefore make the deformation and breakup of the droplets difficult. This effect is more pronounced in the case of spherical nanoparticles.

Thus, knowing the mechanisms behind the morphology stabilization on incorporation of nanoparticles into the immiscible blends, attempts have been made to create blends having optimized properties with respect to the localization of the nanoparticles. In fact, this is the core subject of this book. More discussions on the localization of nanoparticles and its effect on the structure properties of the immiscible blends can be found in Chapters 6–9.

4.6 Conclusion

This chapter has attempted to address the fundamentals of polymer blends with respect to their thermodynamic aspects causing the corresponding phase structures. It has been stated that most polymer pairs are immiscible, leading to phase-separated structures. This feature could be used as an opportunity for manufacturers and researchers to tune structures toward the desired applications. It has been discussed that phase morphology can have a significant effect on the final properties, therefore the study of parameters involved in determination of morphologies is quite important. Some of the influential parameters are blend composition, viscosity/elasticity ratio, processing conditions, as well as interfacial tensions. Considering the different possible morphologies a great deal of effort was made to fabricate and predict the co-continuous morphology owing to its superior characteristics, e.g., mechanical properties over other morphology types. Rheological tools, especially SAOS tests, were found to be quite useful in detecting morphological changes. Co-continuous

blends exhibit a local maxima in their elastic modulus $G'(\omega)$ at low frequencies while droplet−matrix morphologies show a shoulder (plateau modulus) at low-frequency regions. Moreover, it has been shown that co-continuous blends show a tail in their relaxation spectra at longer times (low frequencies) owing to their very large interfacial areas which cannot completely relax within the experimental time. Further, it was discussed that co-continuous structures are thermally unstable and can coarsen during the postprocessing conditions such as annealing which can greatly defect the properties. Therefore, compatibilizers have been used to stabilize the morphologies and mitigate the coarsening effect. Nanoparticles also have been used extensively in the context of stabilization of morphologies. In general, it was discussed that compatibilizers reduce the interfacial tensions and suppress the coalescence and coarsening of the morphologies when they are located at the interface. The efficiencies of the nanoparticles, however, in stabilization were shown to be quite dependent on the localization within the blends.

References

[1] Utracki LA, Weiss RA. Multiphase polymers: blends and ionomers, vol. 395. American Chemical Society; 1989. p. 532.
[2] Paul D, Barlow J. Journal of Macromolecular Science − Reviews in Macromolecular Chemistry and Physics 1980;109:C18.
[3] Paul D, Walsh D, Higgins J. Polymer blends and mixtures. NATO ASI Series E, Applied Science 1985;1.
[4] Niskanen J, Tenhu H. How to manipulate the upper critical solution temperature (UCST)? Polymer Chemistry 2017;8:220−32.
[5] Wu D, Zhang Y, Zhang M, Zhou W. Phase behavior and its viscoelastic response of polylactide/poly(ε-caprolactone) blend. European Polymer Journal 2008;44:2171−83.
[6] Van Puyvelde P, Velankar S, Moldenaers P. Rheology and morphology of compatibilized polymer blends. Current Opinion in Colloid & Interface Science 2001;6:457−63.
[7] Favis BD, Chalifoux JP. Influence of composition on the morphology of polypropylene/polycarbonate blends. Polymer 1988;29:1761−7.
[8] Salehiyan R, Ray SS, Ojijo V. Processing-driven morphology development and crystallization behavior of immiscible polylactide/poly(vinylidene fluoride) blends. Macromolecular Materials and Engineering 2018:1800349.
[9] Favis B, Therrien D. Factors influencing structure formation and phase size in an immiscible polymer blend of polycarbonate and polypropylene prepared by twin-screw extrusion. Polymer 1991;32:1474−81.
[10] Salehiyan R, Ray SS. Processing of polymer blends, emphasizing: melt compounding; influence of nanoparticles on blend morphology and rheology; reactive processing in ternary systems; morphology−property relationships; performance and application challenges; and opportunities and future trends. In: Processing of polymer-based nanocomposites. Springer; 2018. p. 167−97.
[11] Tucker IIIIII, Moldenaers P. Microstructural evolution in polymer blends. Annual Review of Fluid Mechanics 2002;34:177−210.

[12] Fortelný I, Živný A. Film drainage between droplets during theircoalescence in quiescent polymer blends. Polymer 1998;39:2669−75.
[13] Fortelný I, Kovář J, Stephan M. Analysis of the phase structure development during the melt mixing of polymer blends. Journal of Elastomers and Plastics 1996;28:106−39.
[14] Li J, Ma G, Sheng J. Morphological aspects of in-situ compatiblized binary polymer blends with variable viscosity ratios of components. Journal of Macromolecular Science, Part B 2009;48:471−86.
[15] Minale M, Mewis J, Moldenaers P. Study of the morphological hysteresis in immiscible polymer blends. AIChE Journal 1998;44:943−50.
[16] Minale M, Moldenaers P, Mewis J. Effect of shear history on the morphology of immiscible polymer blends. Macromolecules 1997;30:5470−5.
[17] Pötschke P, Paul D. Formation of co-continuous structures in melt-mixed immiscible polymer blends. Journal of Macromolecular Science: Part C: Polymer Reviews 2003; 43:87−141.
[18] RunMing L, Wei Y, ChiXing Z. Phase inversion and viscoelastic properties of phase-separated polymer blends. Polymer Bulletin 2007;59:545−54.
[19] Trifkovic M, Hedegaard A, Huston K, Sheikhzadeh M, Macosko CW. Porous films via PE/PEO cocontinuous blends. Macromolecules 2012;45:6036−44.
[20] Trifkovic M, Hedegaard AT, Sheikhzadeh M, Huang S, Macosko CW. Stabilization of PE/PEO cocontinuous blends by interfacial nanoclays. Macromolecules 2015;48: 4631−44.
[21] Bourry D, Favis B. Cocontinuity and phase inversion in HDBE/PS blends: influence of interfacial modification and elasticity. Journal of Polymer Science Part B: Polymer Physics 1998;36:1889−99.
[22] Gubbels F, Jérôme R, Teyssie P, Vanlathem E, Deltour R, Calderone A, Parente V, Brédas J-L. Selective localization of carbon black in immiscible polymer blends: a useful tool to design electrical conductive composites. Macromolecules 1994;27:1972−4.
[23] Washburn NR, Simon CG, Tona A, Elgendy HM, Karim A, Amis EJ. Co-extrusion of biocompatible polymers for scaffolds with co-continuous morphology. Journal of Biomedical Materials Research 2002;60:20−9.
[24] Avgeropoulos G, Weissert F, Biddison P, Bohm G. Heterogeneous blends of polymers. Rheology and morphology. Rubber Chemistry and Technology Journal 1976;49: 93−104.
[25] Ho R, Wu C, Su A. Morphology of plastic/rubber blends. Polymer Engineering & Science 1990;30:511−8.
[26] Kitayama N, Keskkula H, Paul DR. Reactive compatibilization of nylon 6/styrene−acrylonitrile copolymer blends. Part 1. Phase inversion behavior. Polymer 2000;41: 8041−52.
[27] Omonov T, Harrats C, Groeninckx G, Moldenaers P. Anisotropy and instability of the co-continuous phase morphology in uncompatibilized and reactively compatibilized polypropylene/polystyrene blends. Polymer 2007;48:5289−302.
[28] Everaert V, Aerts L, Groeninckx G. Phase morphology development in immiscible PP/(PS/PPE) blends influence of the melt-viscosity ratio and blend composition. Polymer 1999;40:6627−44.
[29] Krieger IM, Dougherty TJ. A mechanism for non-Newtonian flow in suspensions of rigid spheres. Transactions of the Society of Rheology 1959;3:137−52.
[30] Utracki L. On the viscosity-concentration dependence of immiscible polymer blends. Journal of Rheology 1991;35:1615−37.

[31] Metelkin V, Blekht V. Formation of a continuous phase in heterogenous mixtures of polymers. Kolloidnyi Zhurnal 1984;46:476−80.
[32] Steinmann S, Gronski W, Friedrich C. Cocontinuous polymer blends: influence of viscosity and elasticity ratios of the constituent polymers on phase inversion. Polymer 2001;42:6619−29.
[33] Vanoene H. Modes of dispersion of viscoelastic fluids in flow. Journal of Colloid and Interface Science 1972;40:448−67.
[34] Willemse R, De Boer AP, Van Dam J, Gotsis A. Co-continuous morphologies in polymer blends: a new model. Polymer 1998;39:5879−87.
[35] Ajji A, Choplin L, Prud'Homme RE. Rheology of polystyrene/poly(vinyl methyl ether) blends near the phase transition. Journal of Polymer Science Part B: Polymer Physics 1991;29:1573−8.
[36] Vlassopoulos D. Rheology of critical LCST polymer blends: poly (styrene-co-maleic anhydrite)/poly (methyl methacrylate). Rheologica Acta 1996;35:556−66.
[37] Yu W, Zhou C. Rheology of miscible polymer blends with viscoelastic asymmetry and concentration fluctuation. Polymer 2012;53:881−90.
[38] Épinat C, Trouillet-Fonti L, Sotta P. Predicting phase inversion based on the rheological behavior in polyamide 6/polyethylene blends. Polymer 2018;137:132−44.
[39] Omonov T, Harrats C, Moldenaers P, Groeninckx G. Phase continuity detection and phase inversion phenomena in immiscible polypropylene/polystyrene blends with different viscosity ratios. Polymer 2007;48:5917−27.
[40] Vinckier I, Laun HM. Manifestation of phase separation processes in oscillatory shear: droplet-matrix systems versus co-continuous morphologies. Rheologica Acta 1999;38:274−86.
[41] Yu W, Zhou W, Zhou C. Linear viscoelasticity of polymer blends with co-continuous morphology. Polymer 2010;51:2091−8.
[42] Veenstra H, Verkooijen PCJ, van Lent BJJ, van Dam J, de Boer AP, Nijhof APHJ. On the mechanical properties of co-continuous polymer blends: experimental and modelling. Polymer 2000;41:1817−26.
[43] Palierne J. Linear rheology of viscoelastic emulsions with interfacial tension. Rheologica Acta 1990;29:204−14.
[44] Graebling D, Muller R, Palierne J. Linear viscoelasticity of incompatible polymer blends in the melt in relation with interfacial properties. Journal de Physique IV 1993;3(C7−1525):C1527−34.
[45] Gui Z-y, Wang H-r, Gao Y, Lu C, Cheng S-j. Morphology and melt rheology of biodegradable poly (lactic acid)/poly (butylene succinate adipate) blends: effect of blend compositions. Iranian Polymer Journal 2012;21:81−9.
[46] Maani A, Heuzey M-C, Carreau PJ. Coalescence in thermoplastic olefin (TPO) blends under shear flow. Rheologica Acta 2011;50:881−95.
[47] Stadler FJ. Effect of incomplete datasets on the calculation of continuous relaxation spectra from dynamic-mechanical data. Rheologica Acta 2010;49:1041−57.
[48] Stadler FJ, Bailly C. A new method for the calculation of continuous relaxation spectra from dynamic-mechanical data. Rheologica Acta 2009;48:33−49.
[49] Tschoegl NW. The phenomenological theory of linear viscoelastic behavior: an introduction. Springer Science & Business Media; 2012.
[50] Soo Cho K, Woo Park G. Fixed-point iteration for relaxation spectrum from dynamic mechanical data. Journal of Rheology 2013;57:647−78.

[51] Souza AMC, Demarquette NR. Influence of coalescence and interfacial tension on the morphology of PP/HDPE compatibilized blends. Polymer 2002;43:3959−67.
[52] Macaúbas PHP, Demarquette NR. Morphologies and interfacial tensions of immiscible polypropylene/polystyrene blends modified with triblock copolymers. Polymer 2001; 42:2543−54.
[53] López-Barrón CR, Macosko CW. Rheology of compatibilized immiscible blends with droplet-matrix and cocontinuous morphologies during coarsening. Journal of Rheology 2014;58:1935−53.
[54] Li R, Yu W, Zhou C. Rheological characterization of droplet-matrix versus co-continuous morphology. Journal of Macromolecular Science, Part B 2006;45:889−98.
[55] Li J, Ma G, Sheng J. Linear viscoelastic characteristics of in situ compatiblized binary polymer blends with viscoelastic properties of components variable. Journal of Polymer Science Part B: Polymer Physics 2010;48:1349−62.
[56] Díaz MF, Barbosa SE, Capiati NJ. Improvement of mechanical properties for PP/PS blends by in situ compatibilization. Polymer 2005;46:6096−101.
[57] Shahbazi K, Aghjeh MR, Abbasi F, Meran MP, Mazidi MM. Rheology, morphology and tensile properties of reactive compatibilized polyethylene/polystyrene blends via Friedel−Crafts alkylation reaction. Polymer Bulletin 2012;69:241−59.
[58] Sundararaj U, Macosko C. Drop breakup and coalescence in polymer blends: the effects of concentration and compatibilization. Macromolecules 1995;28:2647−57.
[59] Bandyopadhyay J, Ray SS, Salehiyan R, Ojijo V, Khoza M, Wesley-Smith J. Effect of the mode of nanoclay inclusion on morphology development and rheological properties of nylon6/ethyl−vinyl-alcohol blend composites. Polymer 2017;126:96−108.
[60] Salehiyan R, Song HY, Choi WJ, Hyun K. Characterization of effects of silica nanoparticles on (80/20) PP/PS blends via nonlinear rheological properties from Fourier transform rheology. Macromolecules 2015;48:4669−79.
[61] Elias L, Fenouillot F, Majeste JC, Cassagnau P. Morphology and rheology of immiscible polymer blends filled with silica nanoparticles. Polymer 2007;48:6029−40.
[62] Sinha Ray S, Pouliot S, Bousmina M, Utracki LA. Role of organically modified layered silicate as an active interfacial modifier in immiscible polystyrene/polypropylene blends. Polymer 2004;45:8403−13.
[63] Sinha Ray S, Bousmina M. Compatibilization efficiency of organoclay in an immiscible polycarbonate/poly (methyl methacrylate) blend. Macromolecular Rapid Communications 2005;26:450−5.
[64] Fenouillot F, Cassagnau P, Majesté JC. Uneven distribution of nanoparticles in immiscible fluids: morphology development in polymer blends. Polymer 2009;50:1333−50.
[65] Salehiyan R, Ray S, Bandyopadhyay J, Ojijo V. The distribution of nanoclay particles at the interface and their influence on the microstructure development and rheological properties of reactively processed biodegradable polylactide/poly(butylene succinate) blend nanocomposites. Polymers 2017;9:350.
[66] Zhu Y, Ma H-y, Tong L-f, Fang Z-p. "Cutting effect" of organoclay platelets in compatibilizing immiscible polypropylene/polystyrene blends. Journal of Zhejiang University − Science A 2008;9:1614−20.
[67] Kelnar I, Kratochvíl J, Kaprálková L, Špitálsky Z, Ujčič M, Zhigunov A, Nevoralová M. Effect of graphene oxide on structure and properties of impact-modified polyamide 6. Polymer − Plastics Technology and Engineering 2018;57:827−35.

[68] Kelnar I, Kratochvíl J, Kaprálková L, Zhigunov A, Nevoralová M. Graphite nanoplatelets-modified PLA/PCL: effect of blend ratio and nanofiller localization on structure and properties. Journal of the Mechanical Behavior of Biomedical Materials 2017;71:271−8.

[69] Yousfi M, Livi S, Dumas A, Crépin-Leblond J, Greenhill-Hooper M, Duchet-Rumeau J. Compatibilization of polypropylene/polyamide 6 blends using new synthetic nanosized talc fillers: morphology, thermal, and mechanical properties. Journal of Applied Polymer Science 2014;131:13.